SAVVY Executive Report

savvy
Self-assembled virus-like
vectors for stem cell phenotyping

1. Goal of Project

The **S**elf-**A**ssembled **V**irus-like **V**ectors for Stem Cell Phenot**y**ping (**SAVVY**) project used hierarchical, multi-scale assembly of intrinsically dissimilar nanoparticles to develop novel types of multifunctional Raman probes for analysis and phenotyping of heterogeneous stem cell populations.

Human stem cells have great potential for a broad range of therapeutic and biotechnological applications, such as regenerative medicine or pharmaceutical testing, but the characterization or sorting of stem cell populations has been extremely challenging and is generally addressed using flow cytometry. However this approach is vitally hampered by: (i) lack of specific antibodies, (ii) need for fluorescence markers that limit multiplexing, (ii) low concentration of stem cells in the abundance of background cells, (iv) low efficiencies and high costs due to need for antibodies. The SAVVY approach uses intrinsic differences in the composition of cell membranes to distinguish and ultimately sort stem cell populations.

Compared to the current practice (e.g., fluorescence-based multiplexing), **SAVVY** uses a fundamentally different approach, which (i) does not require antibodies, aptamers, or any other biomarker, (ii) is fluorescence-label free, and (iii) is thus scalable at acceptable cost. Because of the fundamental differences to the currently used antibody-based detection schemes, **SAVVY** provides a paradigm shift for stem cell phenotyping with applications in medical diagnostics.

The proposed integrated live cell sorting system incorporates nanoparticle-based signal enhancers along with Raman micro-spectroscopy in an integrated microfluidic cell sorter (‘**SAVVY sorter**’). This requires preparation of fundamentally novel Raman probes (‘**SAVVY reporter**’) based on the design and hierarchical self-assembly of constituent nanoparticles.

This project integrated a number of nanoscale components via hierarchical self-assembly into Raman active particles and evaluated their usability in cell sorting applications. Most importantly, we made excellent progress towards the nanoscale self-assembly of a complex array of functional nanoparticles at multiple length scales. The base particle architecture was achieved by an electrohydrodynamic co-jetting process that can produce Janus vectors with distinct hemispheres (i.e., the compartments). In this design, both the interior as well as the surfaces of the vector’s hemispheres can be controlled independently. Anisotropic surface-directed self-assembly of amphiphilic gold NP onto the Janus vectors constituted another critical component. The remaining surface area of the vector particles is modified with polyethylene-glycol to impart particle stealth. The third functional element in the form of plasmonic nanostars ensures high Raman-enhancement (SERS).

In parallel, excellent progress was made towards establishing human pluripotent stem cell cultures and appropriate differentiation protocols in formats that are directly accessible by Raman microspectroscopy. We successfully established all functional process steps of the

microfluidic-based system, such as particle/cell separation, cell singularization, Raman analysis and cell sorting and translated them into independent microfluidic modules. These single modules were successfully characterized and one module for each functional step was selected as the preferred design.

Even though WITec joined the consortium only during month 19 of the project, a prototype of the cell sorter with line illumination was successfully built by WITec. The initial Raman results support the overall feasibility of the SAVVY cell sorting concept: (i) It could be shown that a very low laser power is sufficient to obtain reasonably good Raman signals, even for short integration times. (ii) We confirmed enhancement of the Raman signal of 1-2 orders of magnitude as compared to unlabeled particles. (iii) Although the final step of a fully integrated hardware system comprised of the microfluidic chip AND the microscope in one unit was not realized, we still could distinguish two different cell types based on their Raman signature inside of a microchannel.

While this project has validated the fundamental approach taken by the SAVVY consortium, further engineering work would be necessary to establish an integrated hardware solution that would be sufficiently robust for larger-scale cell sorting.

2. Component Fabrications for the SAVVY Reporter

The design of the SAVVY reporters is comprised of a core 500 nm particle immobilized with rippled nanoparticles for cell attachment and nanostars for SERS enhancement. As such, below are the three individual components that were designed, fabricated, and characterized for the final assembly: (i) rippled nanoparticles, (ii) nanostars, (iii) and Janus particles.

2.1 Synthesis of Rippled Nanoparticles

To synthesize rippled nanoparticles, an alcohol-based process has been established that works at room-temperature and allows for mechanical mixing. After developing the synthetic protocol that gives consistent characteristics of nanoparticles in terms of surface monolayer and size, we tried to scale up the synthesis to get 1 g per synthesis. One of the key parameter in the synthesis is the mixing of the solution prior to addition of reducing agent. Vigorous mixing with big stirring bars in round bottom flasks could easily overcome that barrier to get homogeneous distribution of the precursors. The characterization of the striped nanoparticles at a small-scale and a large-scale synthesis has been compared in terms of size and ligand ratio. The comparison, shown in **Figure 1** and **Figure 2**, revealed that there is no significant difference between the two synthetic approaches. The approach of large batch synthesis and parallel reactors is therefore viable.

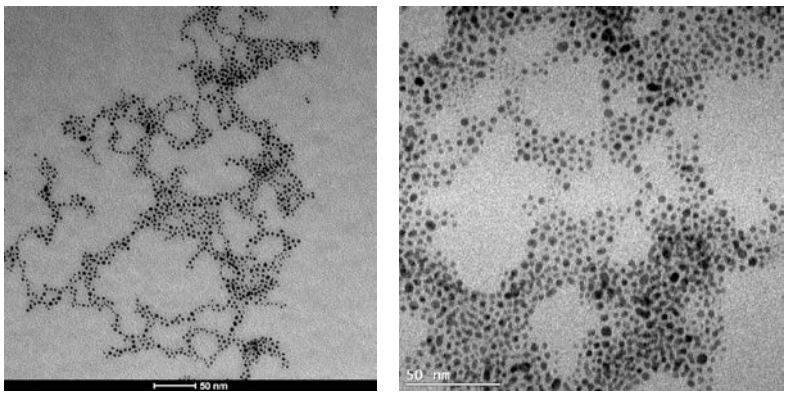

Fig. 1: *TEM images of the particles from 1 g synthesis (left) and 0.1 g synthesis (right)*

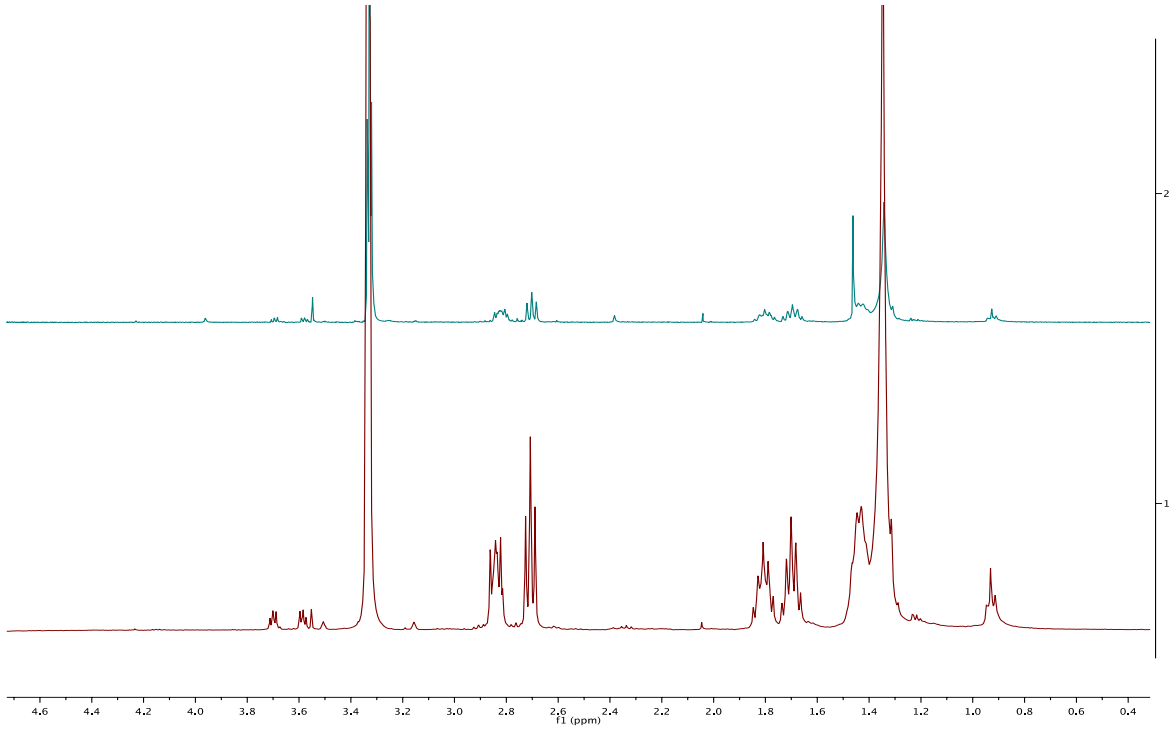

Fig. 2: *^{1}H NMR spectroscopy of ligands after chemically etching of striped particles. The ratio of peaks 0.93 ppm and 1.87-1.65 ppm is similar to 0.1 g synthesis (above) for 1 g synthesis (below).*

As explained in the synthesis protocols, for the preparation of a SAVVY reporter, the amount of rippled particles is not the limiting step. Less than a milligram could be enough for testing a couple of milligrams of polymer beads and nanostars. The small size of the rippled nanoparticles implies higher concentration (higher number of nanoparticles for a given volume), even for a small amount of mass. The current protocol that yields 1 g of nanoparticles per day would be more than enough for massive production of SAVVY reporters for the future. Details regarding the synthesis of the rippled nanoparticles are below.

Striped nanoparticles have been produced with 11-mercaptoundecane sulfonate and 1-octanethiol, as shown in a simple scheme in **Figure 3**. To this mixture, gold salt ($HAuCl_4$) in ethanol and the thiol ligands in methanol were added, followed by a saturated solution of sodium borohydride ($NaBH_4$) in ethanol. After sedimentation overnight, the nanoparticles were washed by centrifugation several times with ethanol, methanol, and acetone consecutively. Finally the precipitate was left under vacuum to dry completely.

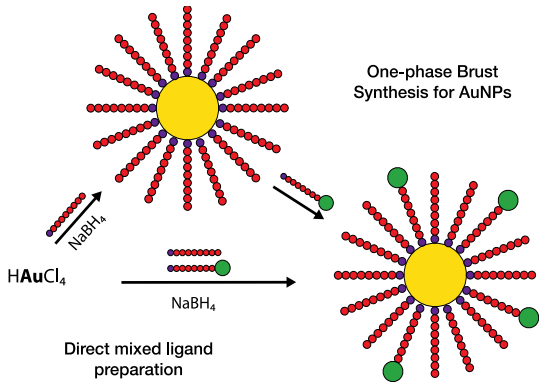

Fig. 3: *Synthesis scheme for the fabrication of rippled nanoparticles.*

Rippled nanoparticle could also be specifically synthesized to contain desired ligands (such as *N*-hydroxysuccinimide, amine carboxylic acid or azide ended thiol ligands), which allowed the application of different chemistries for the attachment to nanostars and polymeric particles, as depicted in **Figure 4** below.

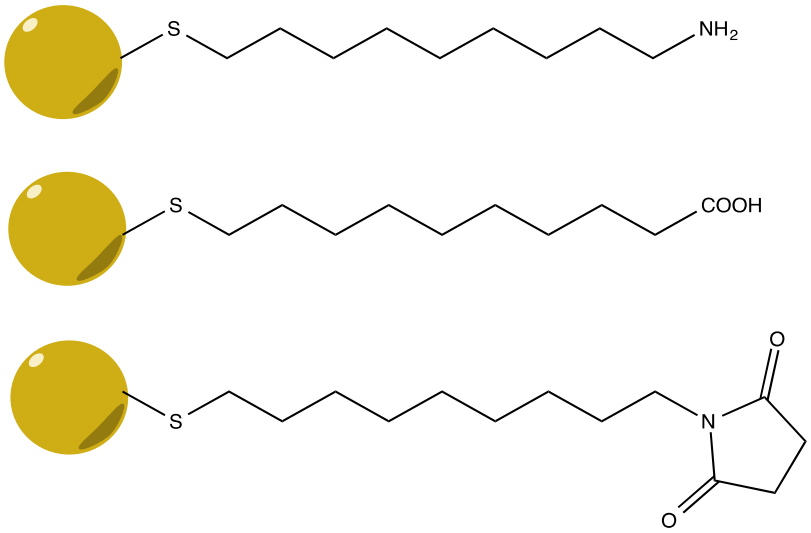

Fig. 4: *Schematic representation of functional ligands used for pole functionalization of striped nanoparticles.*

During synthesis, gold nanoparticles are formed as heterogeneous mixtures of different sizes and ligand densities. This leads to part of the batch being poorly covered with water-soluble ligands and thus, agglomerating and being insoluble in water. Therefore, it is sometimes necessary to purify the nanoparticles from poorly soluble aggregates and even nanoparticles that have very big or very small sizes. To achieve this goal, we apply a density gradient ultracentrifugation method also known as fractionation. The technique is widely used among protein biochemists and cell biologists to purify proteins or separate cellular compartments from each other. The procedure used for this fractionation and some sample TEM images of the particles before and after the fractionation are demonstrated in **Figure 5** below. Analytical ultracentrifugation (AUC) was used to separate the gold nanoaparticles by sizes (**Figure 6**). Transmission electronic microscopy (TEM) analysis confirmed the monodispersed nanoparticle fractions obtained (**Figure 7**).

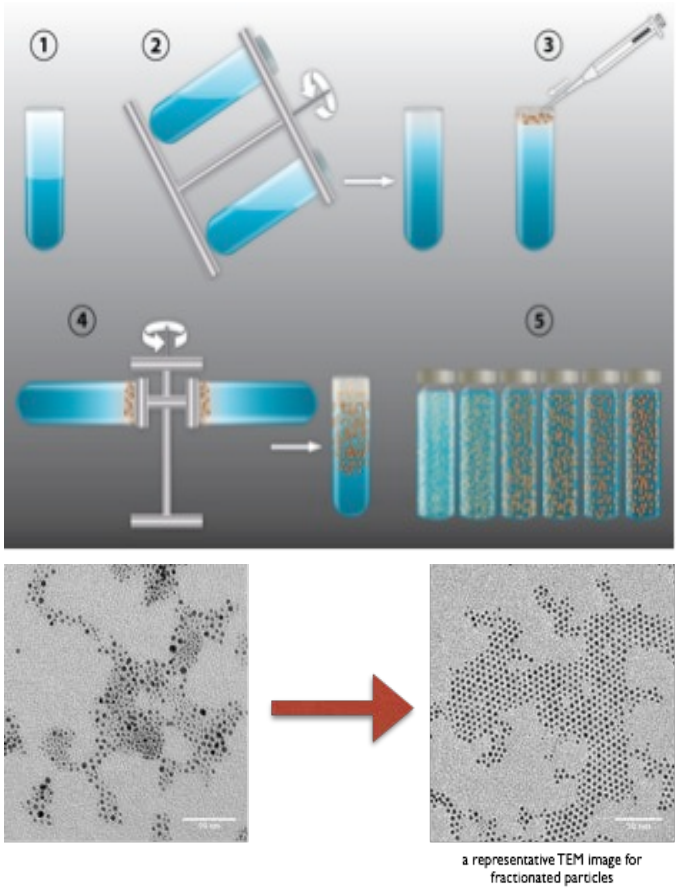

Fig. 5: *Schematic explanation of density gradient ultracentrifugation protocol and sample TEM images of the rippled nanoparticles before (left) and after (right) fractionation.*

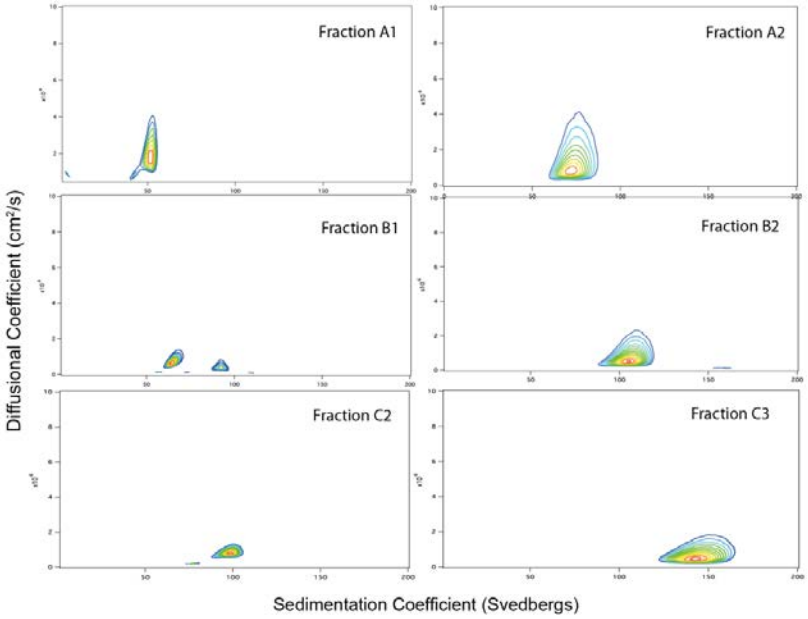

Fig. 6: *2D Sedimentation Data for different fractions of striped nanoparticles. Unimodal distribution plots confirms successful separation of the striped nanoparticles*

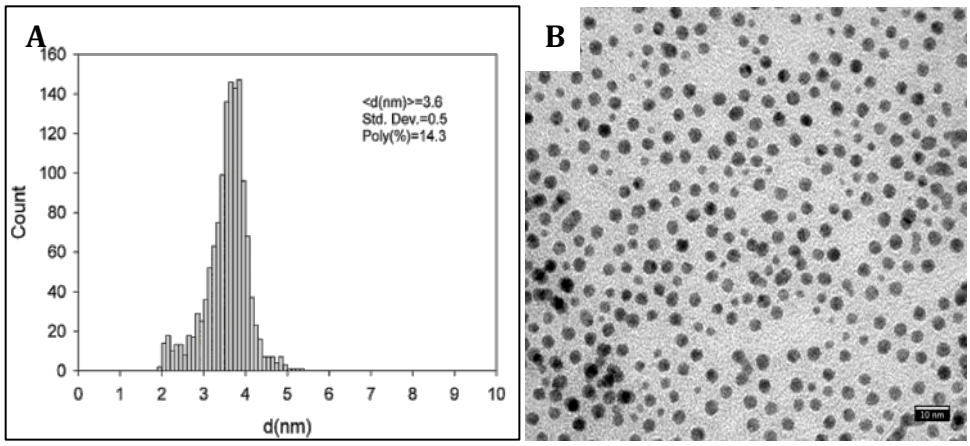

Fig. 7: *Size distribution (**a**) and TEM image (**b**) of RNPs used for SAVVY reporter assembly.*

A mixture of hydrophilic and hydrophobic organic molecules is used to cover the surface of small gold nanoparticles through gold – sulfur bonds. During functionalization of gold nanoparticles the same chemistry is used binding gold and sulfur. This implies a similar kinetics for functional ligands and MUS/OT ligands that are mainly covering the surface. Therefore, it can be safely assumed that storage quality of the nanoparticles does not alter upon functionalization. The characterization of functional groups on gold nanoparticles is conducted by NMR. The peaks are assigned to each corresponding molecule and quantitative estimation is conducted based on the integrations of the peaks shown in **Figure 8**. 10:1 molar ratio (MUSOT:N3 linker) is consistently found over three replications of functionalization experiments.

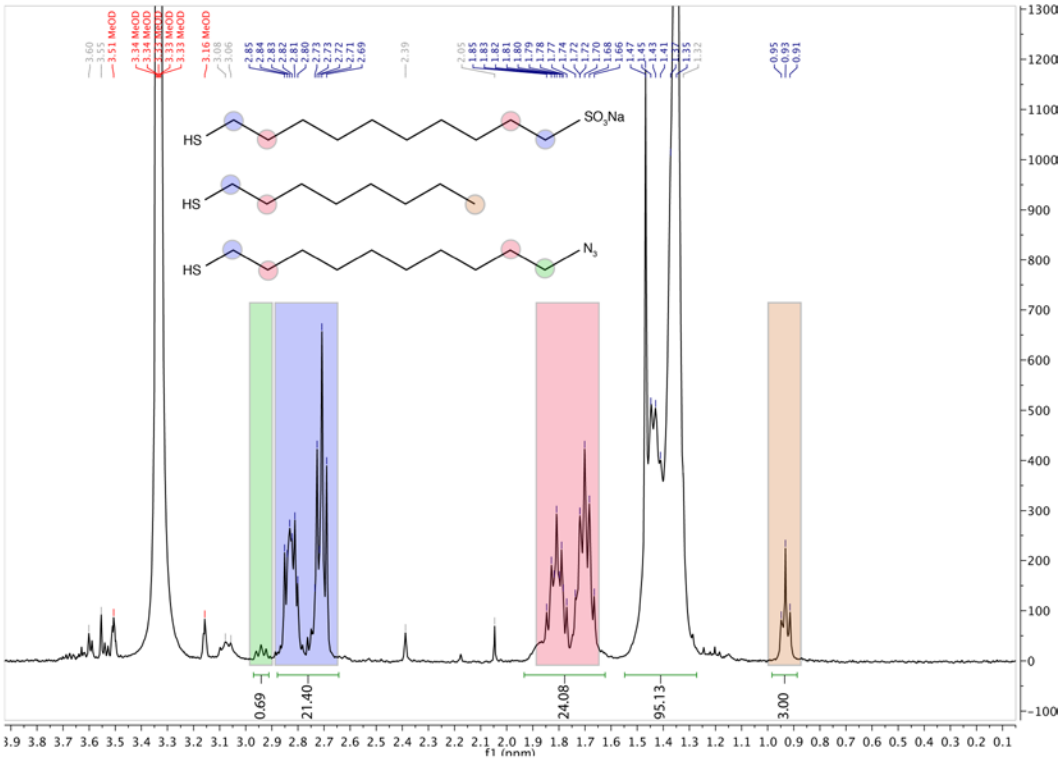

Fig. 8: *NMR spectrum of mixed monolayer gold nanoparticles with MUS and OT after functionalization with azide linker.*

2.2 Synthesis of Nanostars

The approach here was to work on a 100 mg batch synthesis of gold nanostars (AuNSs) and use an increase in reaction volume as a scale-up-strategy. 30 mg of gold nanostars can be obtained using 500 mL synthesis. The performance of several syntheses per day or the increase of the volume per synthesis, are two viable methods for obtaining the desired amount of gold nanoparticles. Fabrication details are provided below.

AuNSs were prepared by a modified seed-mediated growth method. Briefly, the seed solution was prepared by adding a citrate solution to $HAuCl_4$ solution under vigorous stirring. After a brief boiling period, the solution was cooled down to room temperature and kept at 4 °C for long-term storage. The as-synthesized Au nanoparticle seeds had an LSPR maximum at 519 nm. For AuNSs synthesis, citrate-stabilized seed solution was added to $HAuCl_4$ solution containing HCl in a glass vial at room temperature under moderate stirring. Quickly, $AgNO_3$ and ascorbic acid were added simultaneously to the above solution. The solution rapidly turns from light red to green indicating the formation of AuNSs. Immediately after synthesis, the solution was stirred with PEG-SH, washed by centrifugation, and redispersed in water. The synthesized AuNSs present a main Localized Surface Plasmon Resonance (LSPR) located around 750 nm and a less intense shoulder at lower wavelengths, corresponding to the contributions of the tips and the nanostar core, respectively (**Figure 9**). A TEM image of the AuNSs obtained is depicted in Figure 9b. Gold nanoparticles, which feature multiple sharp tips and present core sizes around 35 nm, were successfully obtained.

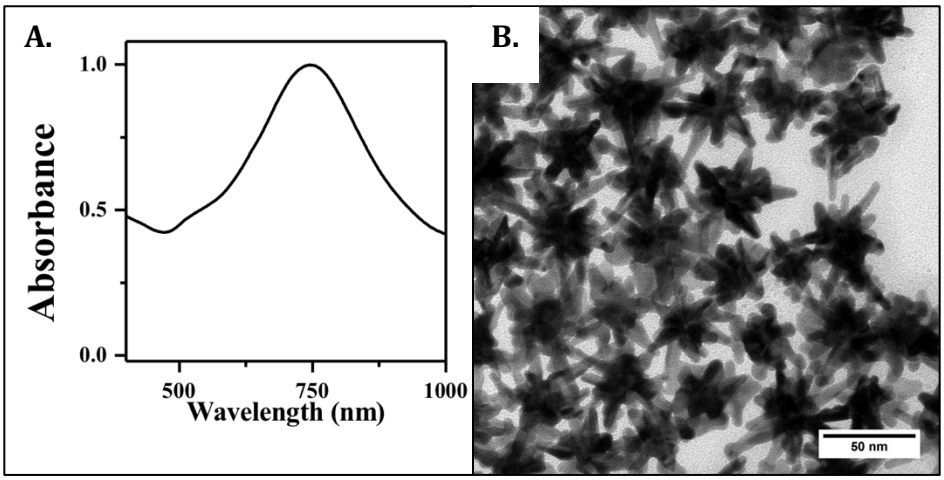

Fig. 9: *UV-Vis spectra (**a**) and TEM image (**b**) of AuNSs*

To functionalize the AuNSs with azide groups, the AuNS were incubated overnight with N_3-PEG-NH_2 after the washes, in order to target a theoretical surface modification of 95 molecules per nm^2. This amount of ligand per nm^2 should ensure surface saturation, as previously reported.[1] Typically, gold nanoparticle functionalization requires the removal of free ligands after reaction. While more sophisticated separation methods are needed for clusters or small nanoparticles, for larger gold nanoparticles such as gold nanostars, washing by centrifugation is a well-known procedure to eliminate the unreacted ligands.[2] After functionalization the particles were stable, as confirmed by the UV-Vis spectra and the TEM characterization (**Figure 10**). Since further steps, which mainly involve click reaction with PLGA nanoparticles, has not been affected by the possible lack of reproducibility of the AuNS

functionalization, we consider this a good strategy to properly modify the gold surface of the plasmonic nanoparticles.

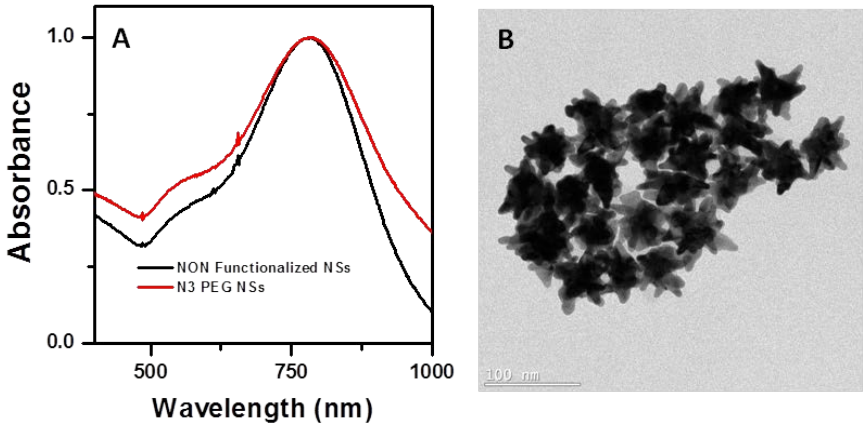

Fig. 10: A) *UV-Vis spectra of non functionalized AuNSs (black) and azide-modified (red) AuNSs.* ***B)*** *TEM image of AuNSs after functionalization with N_3-PEG-NH_2.*

2.3 Fabrication of Janus Particles

The goal in this section of the project was to fabricate Janus particles with distinct patches that could be used for the immobilization of gold nanostars and rippled nanoparticles. The particles were fabricated using the Electrohydrodynamic (EHD) Co-Jetting procedure developed and were analyzed with several different characterization tools, including SEM, confocal microscopy, NTA, and DLS before being used to create the SAVVY assemblies. The details of the fabrication and characterization of the Janus vectors are below.

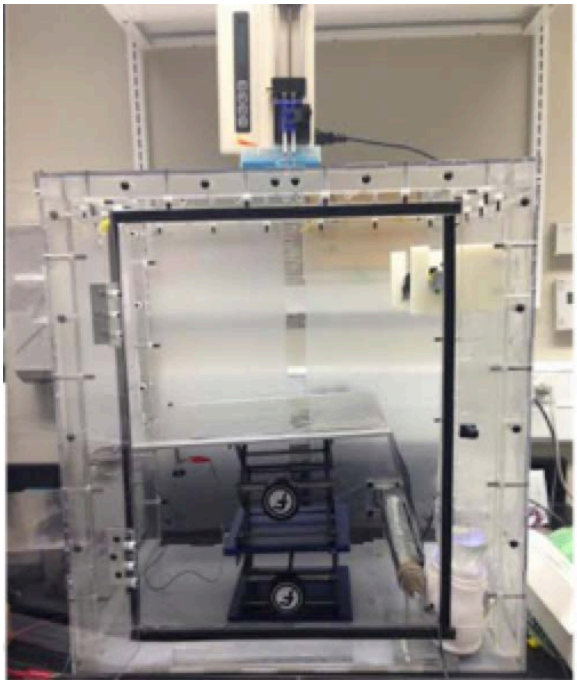

Fig. 11: *Scaled up Electrohydrodynamic (EHD) Co-Jetting station with conveyor belt.*

PLGA particles were fabricated through the EHD co-jetting procedure (**Figure 11**), as previously established in the Lahann group.[3-5] Briefly, during EHD co-jetting polymer solutions are pumped through syringes tipped with metal needles in a laminar regime, while an electric field is applied to the needles. The solutions form a Taylor cone at the tip of the needles and from this droplet a polymeric jet is ejected towards the collecting electrode. The jet splits into a spray of droplets, where the solvents evaporate rapidly, leaving behind polymeric particles on the counter electrode. In order to fabricate particles on a gram basis, a roll-to-roll system for the EHD co-jetting was designed that is capable continuously synthesizing nanoparticles (Figure 11). Based on this system, we are able to fabricate 0.5 g of nanoparticles per hour, for a total of 50 grams per day, which easily supersedes the requirements of this project. To collect and purify these particles for further studies, the particles were collected in sterile DI water with tween 20 and

fractionated via centrifugation into more monodispersed populations. The formulation of the Janus particles, a SEM image of the Janus particles after collection, and their size distribution measurements after the purification via DLS (Dynamic Light Scattering) are demonstrated in **Figure 12.**

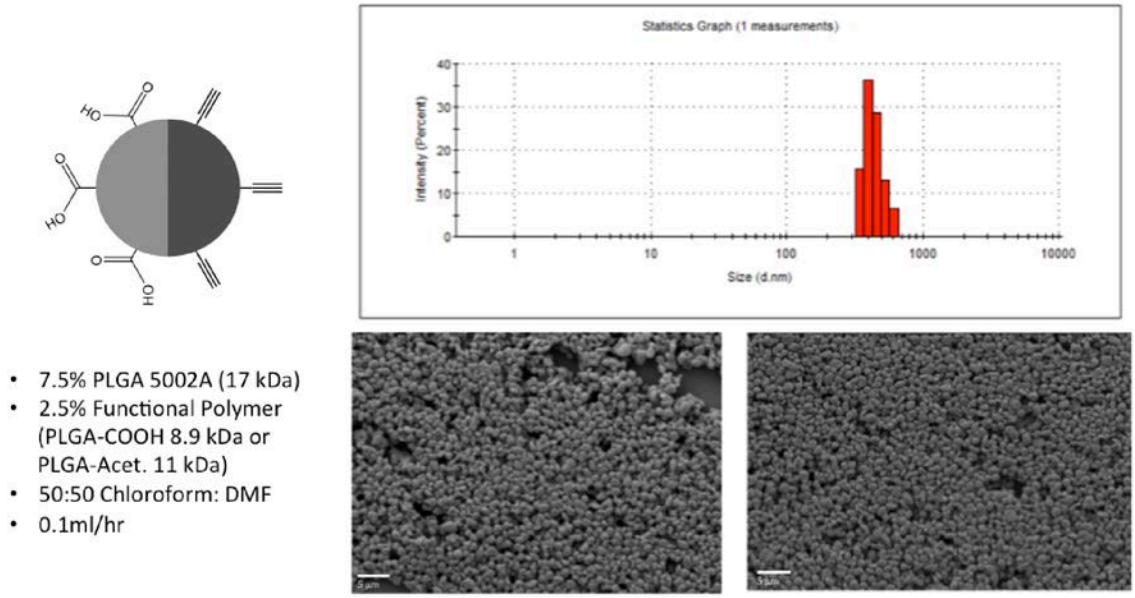

Fig. 12: *Schematic of the Janus particles containing different functional polymers in each side, the formulation used for the fabrication, their SEM after fabrication, and size distribution via DLS analysis.*

Through various experiments, it has been determined that the best methods for Quality Control (QC) of the Janus particles before/after surface modification/immobilization is to test each batch with SEM/TEM and DLS to determine their size distribution, shape, and level of nanoparticle immobilization. A sample of QC for a specific batch is demonstrated in **Figure 13**.

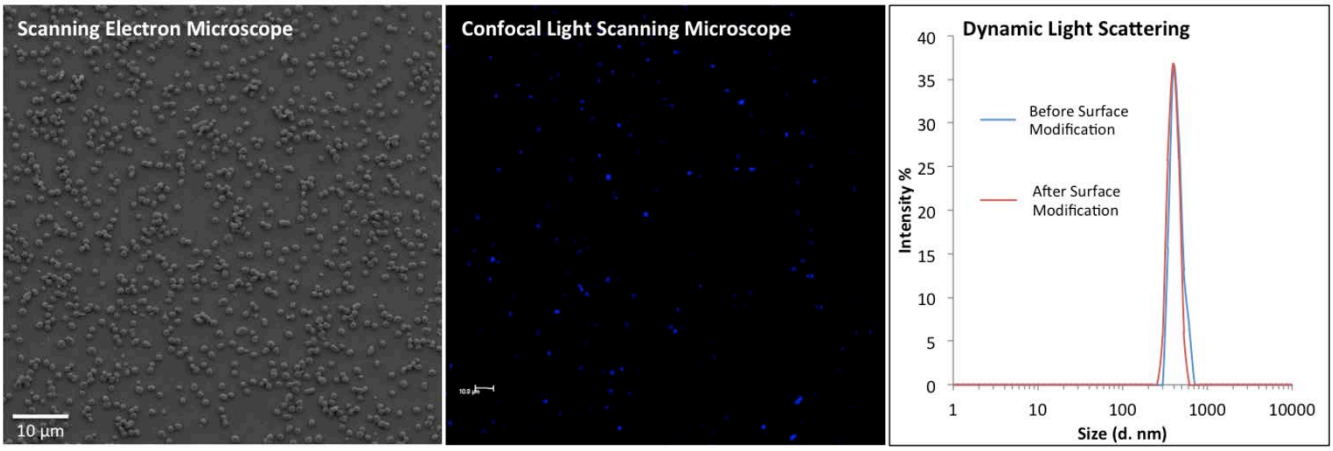

Fig. 13: *QC control of Janus vectors for a batch based on SEM, CLSM, and DLS analysis of the particles.*

In order to quantify the ligand density on the surface of the particles, a procedure established by the Lahann lab was used (Rahmani, et al, 2015 Journal of Drug Targeting).[6] Nanoparticles with an alkyne functional group on the surface were fabricated using the EHD co-jetting technique. After centrifugation, the particles were characterized with Nanosight to determine their size distribution as a function of their concentration and were then reacted with

different amounts of azide-PEG-FITC via copper catalyzed click chemistry overnight. The nanoparticles were centrifuged to separate the particles from the unreacted material and the unreacted azide-PEG-FITC was isolated and measured via UV Visual Spectroscopy to determine the amount of unreacted material based on a previously established calibration curve. Based on this information, as well as on the size distribution and concentration measurements, the total number of PEG molecules reacted per surface area of the nanoparticles was determined. Here, two sets of particles, one set with functional groups on both hemispheres (i.e., monocompartmental) and one set with functional groups just on one side (i.e., bicompartmental) were used. **Figure 14** illustrates this data for both monocompartmental and bicompartmental nanoparticles for three different concentrations of the azide-PEG-FITC molecule. In the case of the monophasic particles, the ligand density increased with increasing PEG concentrations. The same trend was observed for the bicompartmental nanoparticles, with the distinction that at higher concentrations the ligand density of the bicompartmental nanoparticles is significantly lower (3.67 ligands per squared nanometer) due to the fact that only one hemisphere is covered with the ligand.

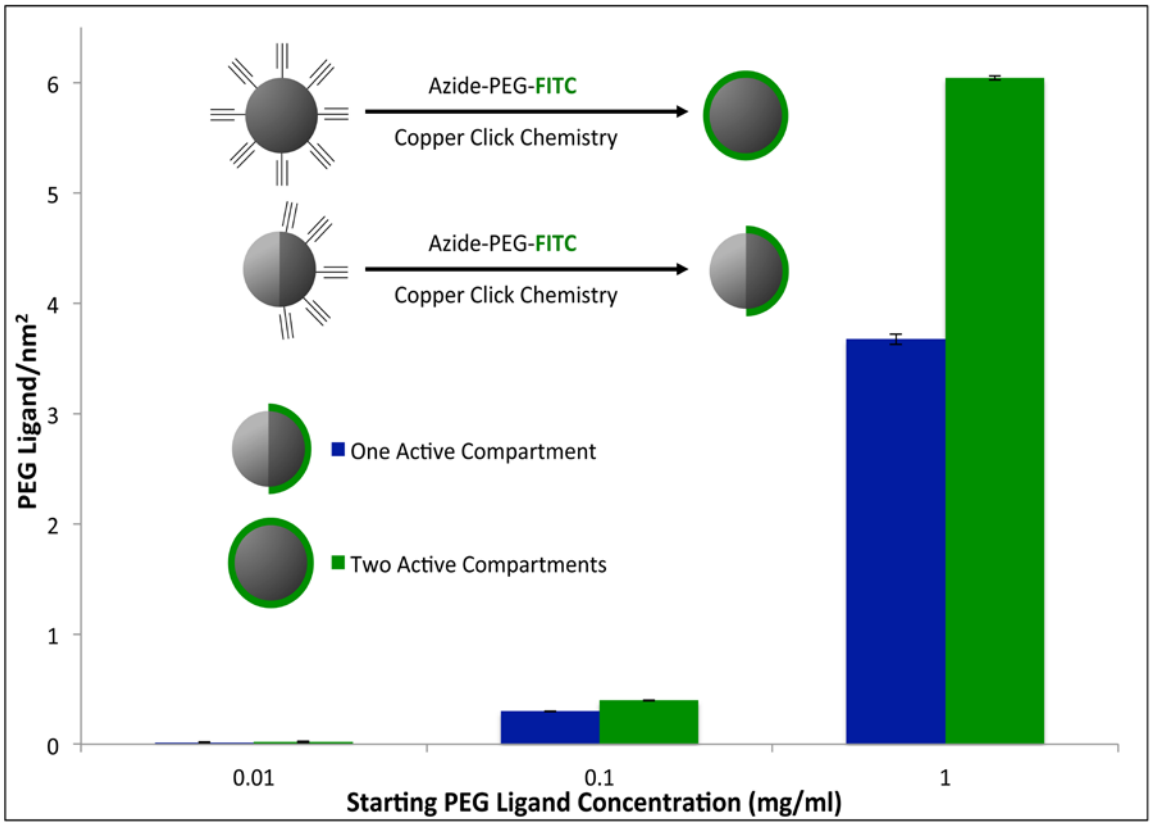

Fig. 14*: Determining PEG density on the surface of nanoparticles. Monophasic or Janus particles with a functional polymer on the entire surface or one hemisphere, respectively, were reacted with azide-PEG-FITC and the PEG ligand per area was determined for each.*

To determine the best methods for the handling and storage of the Janus particles, several approaches have been examined. For short-term storage, the particles can be kept in a 4^{o}C storage unit for up to 1 month before use in cellular experiments. Based on SEM imaging and DLS, such particles retain their shape, morphology, immobilization, and size distribution for this period. It is recommended that the particles be briefly tip sonicated and tested with DLS

before each use. For long-term storage, the Janus particles need to be freeze-dried after the various immobilization steps and stored in the freezer. To use, the particles can simply be resuspended in DI water and tween 20, briefly tip sonicated, and used. As a precautionary step, the particles should be analysed via DLS to ensure their successful resuspension. Based on recent analysis, the freeze-drying of particles does not harm the particles and results in well dispersed particles upon resuspension. As demonstrated in **Figure 15**, the particles retained their average size and concentration after the freeze-drying step.

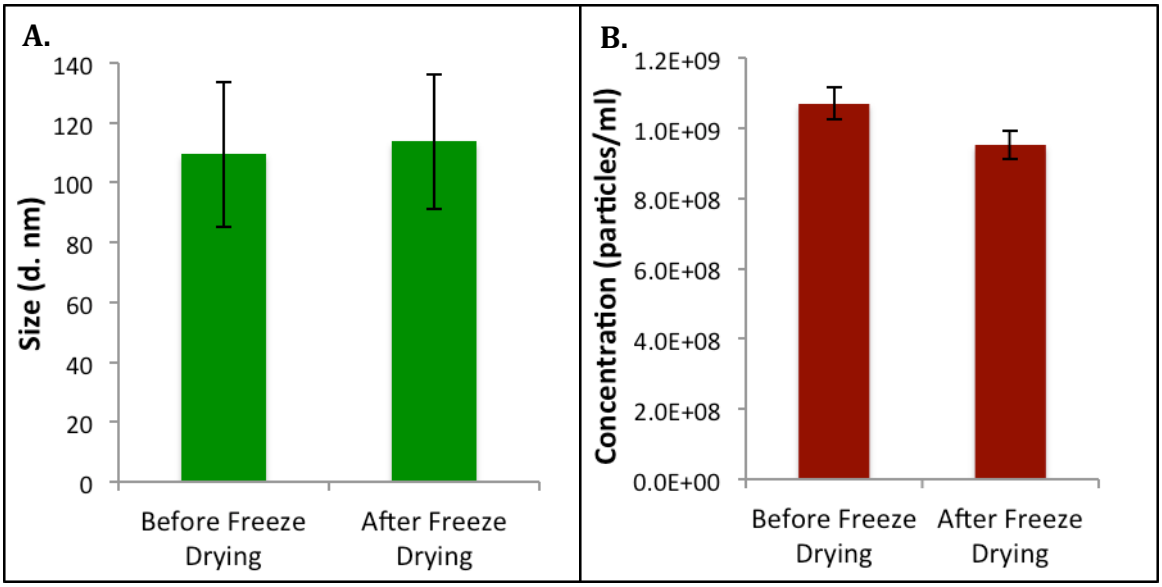

***Fig. 15**: Particle characterization with NTA to before and after freeze-drying. (A) Demonstrates the consistent size distribution of the particles and (B) the concentration before and after freeze-drying for storage.*

3. Assembly of SAVVY Reporters

Once the individual components of the SAVVY reporter were fabricated, their assembly into the SAVVY reporters were investigated. Two approaches were pursued, where one involved using polystyrene (PS) beads as the particle to immobilize the rippled nanoparticles & nanostars on, and the second used the Janus particles discussed above for the immobilization. Both approaches are discussed in detail below.

3.1 PS Assemblies

The hierarchical assembly of the SAVVY components using the PS beads is illustrated in **Figure 16**.

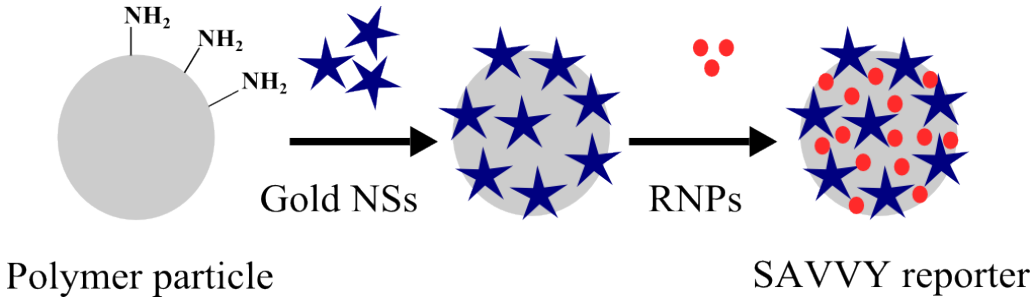

***Fig. 16**: Sketch of the assembly of amino-polymeric PS particles with gold nanostars (NSs) and rippled gold nanoparticles (RNPs).*

Amino-functionalized polystyrene (PS) particles can react with gold nanostars and rippled gold nanoparticles. The high affinity of gold and the amino groups led to a particularly stable structure. The non-detachment of the gold nanoparticles from the polymer surface in the presence of cell culture medium confirmed the strong interaction between the particles and the nanostars (**Figure 17**).

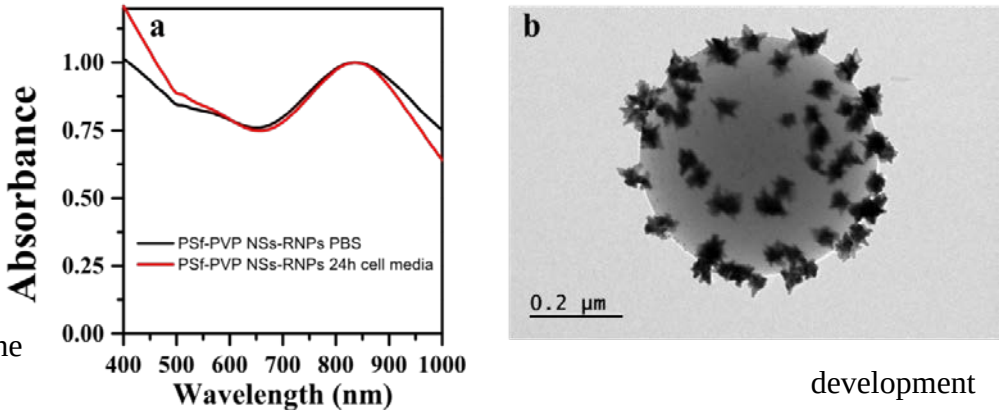

***Fig. 17**: UV-VIS spectra of PSf-PVP NSs-RNPs assembled in PBS (black) and after 24h in cell culture medium (red). b) TEM image of the assembled structure after 24h in cell culture medium.*

The development of a strategy to modify the loading of nanostars onto the microparticles was also carried out. For PS beads, by keeping constant the amount of gold nanostars and decreasing the final concentration of the polymeric particles, we were able to obtain polymer particles covered with gold nanostars as shown in **Figure 18**.

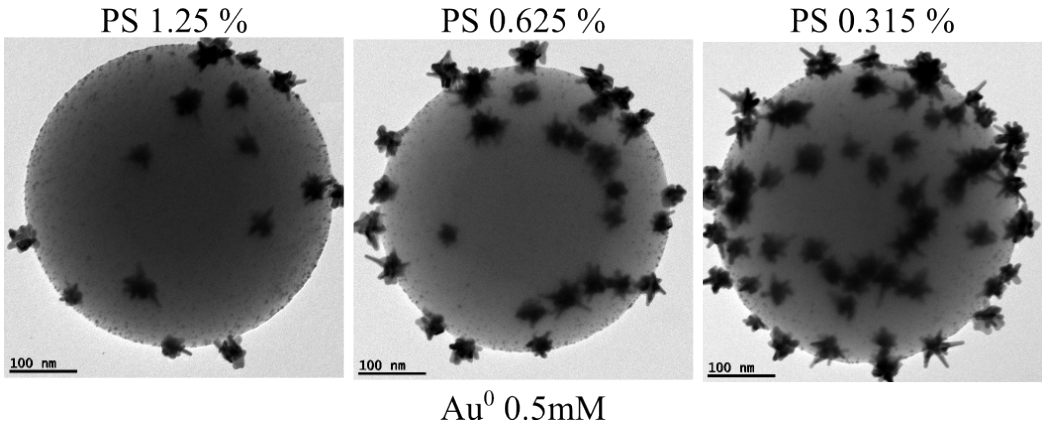

***Fig. 18**: TEM images of PS beads covered with different amount of gold nanostars and rippled nanoparticles.*

In conclusion, we have developed several strategies to obtain different coverage of gold nanostars onto the polymer surface. Cellular uptake experiments have been conducted using the hierarchical assembly of SAVVY reporters with the combination of amounts that give the best coverage and stability. HeLa cell lines were used for these experiments and the assembly was incubated with the cells at 37 °C for 1 hour. Confocal microscopy images showed that the assembly incorporated successfully within the cell membranes. While PS beads - nanostars assembly samples showed only background fluorescence, the addition of striped nanoparticles clearly proved the presence of SAVVY assembly on the cells as seen in **Figure 19**.

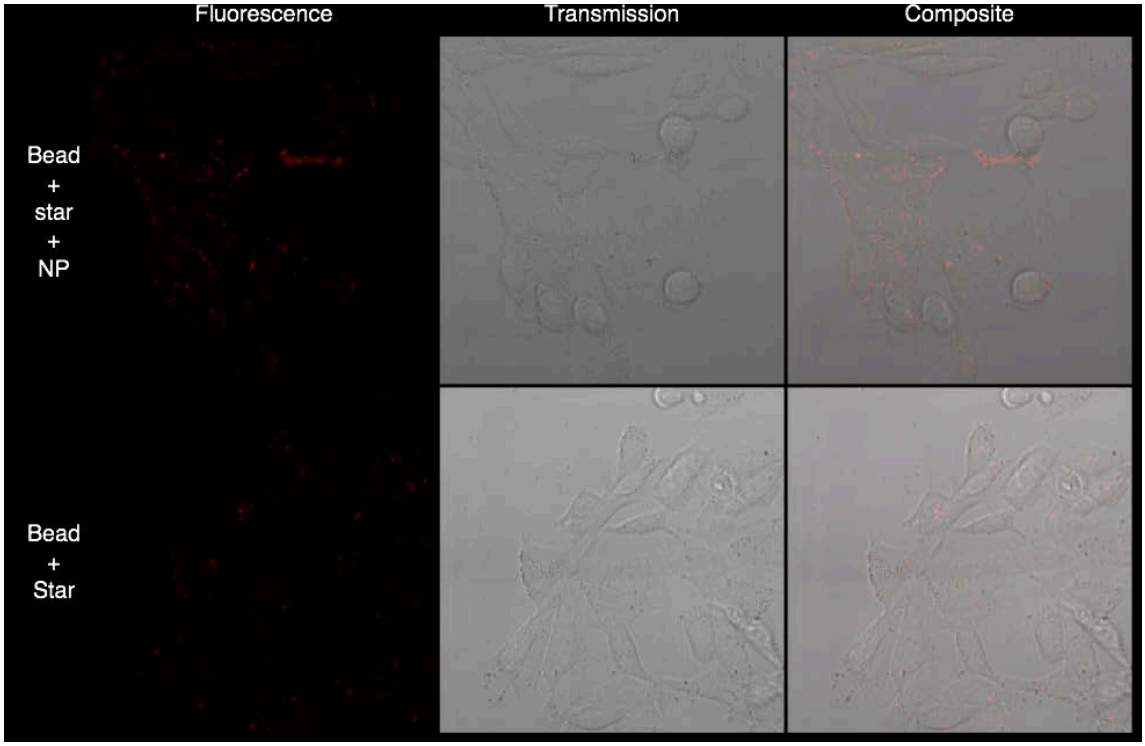

***Fig. 19**: Confocal microscopy images of SAVVY assembly and control assembly with no striped nanoparticles clearly show the difference in fluorescence and particle concentration around the cells.*

Janus Assemblies

To fabricate Janus particles for covalent immobilization of the rippled NP and nanostars, one side of the particles needed to contain alkyne groups, while the second side needed to contain groups to reduce the non-specific association. As such, the particles were used to immobilize a hydroxyl star-PEG to the hemisphere containing the carboxyl groups via EDC/sulfo-NHS chemistry to reduce the non-specific attachment of the SAVVY reporters, while

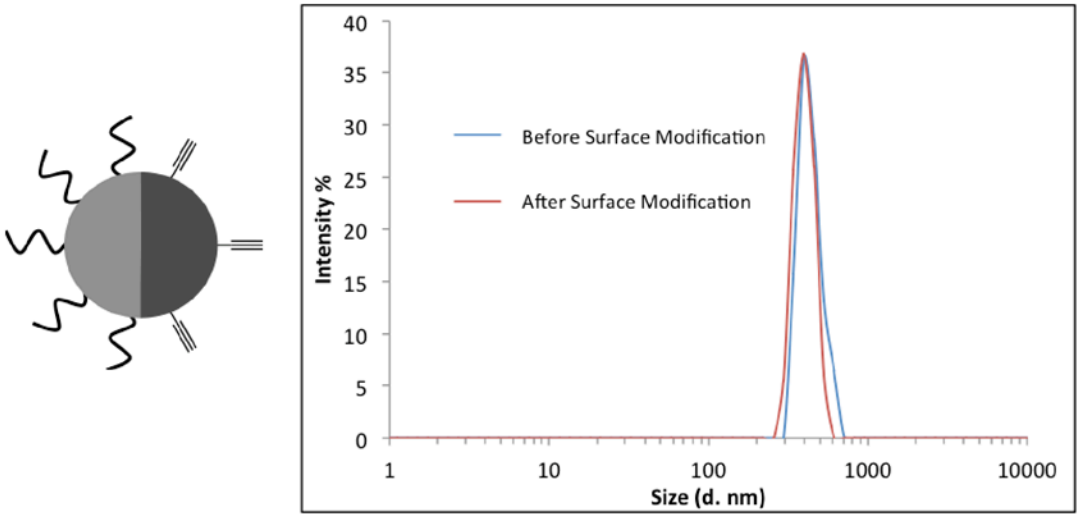

***Fig. 20**: Schematic of the Janus particles used for the covalent attachment of SAVVY reporters and their size distribution before and after the surface modifications.*

thesecond hemisphere containing the PLGA-alkyne groups were left unmodified (**Figure 20** contains a schematic of these particles after surface modification).

The particles were analyzed with DLS to determine their size distribution before and after the surface modification (Figure 20), which demonstrated a consistent size of about 500 nm (the final size of particles was at 580 nm). As can be seen, the size distribution narrows after the surface modification as the particles tend to aggregate less after PEG-ylation. Copper catalyzed click chemistry was then used to immobilize nanostars and rippled nanoparticles on the second hemisphere.

For the immobilization of the gold nanostars, the Janus particles containing PEG on one hemisphere were incubated with nanostars functionalized with an azide-PEG, washed, and imaged via SEM and STEM to determine the selective immobilization of the stars on one hemisphere. While the concentration of the Janus particles and the nanostars, as well as the washing steps, were optimized, a formulation was developed for the selective immobilization of the gold nanostars on one patch as demonstrated in **Figure 21**.

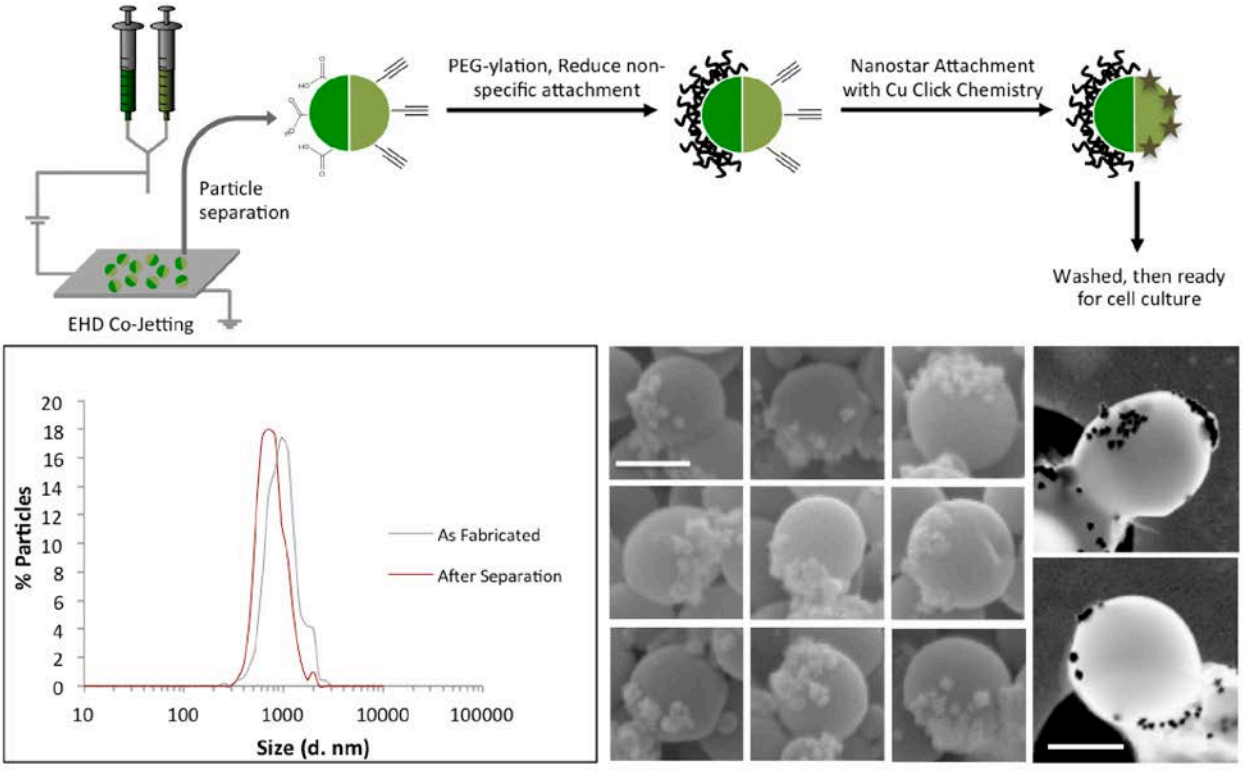

Fig. 21*: Schematic for the processing of the Janus particles, their size distribution before and after preparation, and selective SEM and STEM images of the particles with gold nanostars immobilized on one hemisphere.*

The same strategies as with the nanostar attachment were used for the immobilization of rippled nanoparticles on the Janus particles. Janus particles containing alkyne groups on one side and carboxyl groups on the second side were fabricated using EHD co-jetting. The particles were fractionated into 500 nm particles via serial centrifugation and analyzed via dynamic light scattering (**Figure 22)**. The particles were PEG-ylated on the carboxyl side via EDC/sulfo-NHS chemistry with an eight-arm amine PEG. For the immobilization of amphiphilic nanoparticles, PEG-ylated Janus vectors were incubated with the amphiphilic NPs functionalized with azide

groups, washed multiple times to remove all unreacted material, then imaged via TEM imaging to determine their selective immobilization (**Figure 22**). Additional images of Janus particles with the amphiphilic nanoparticles on one side as TEM quantification are displayed in **Figure 23**.

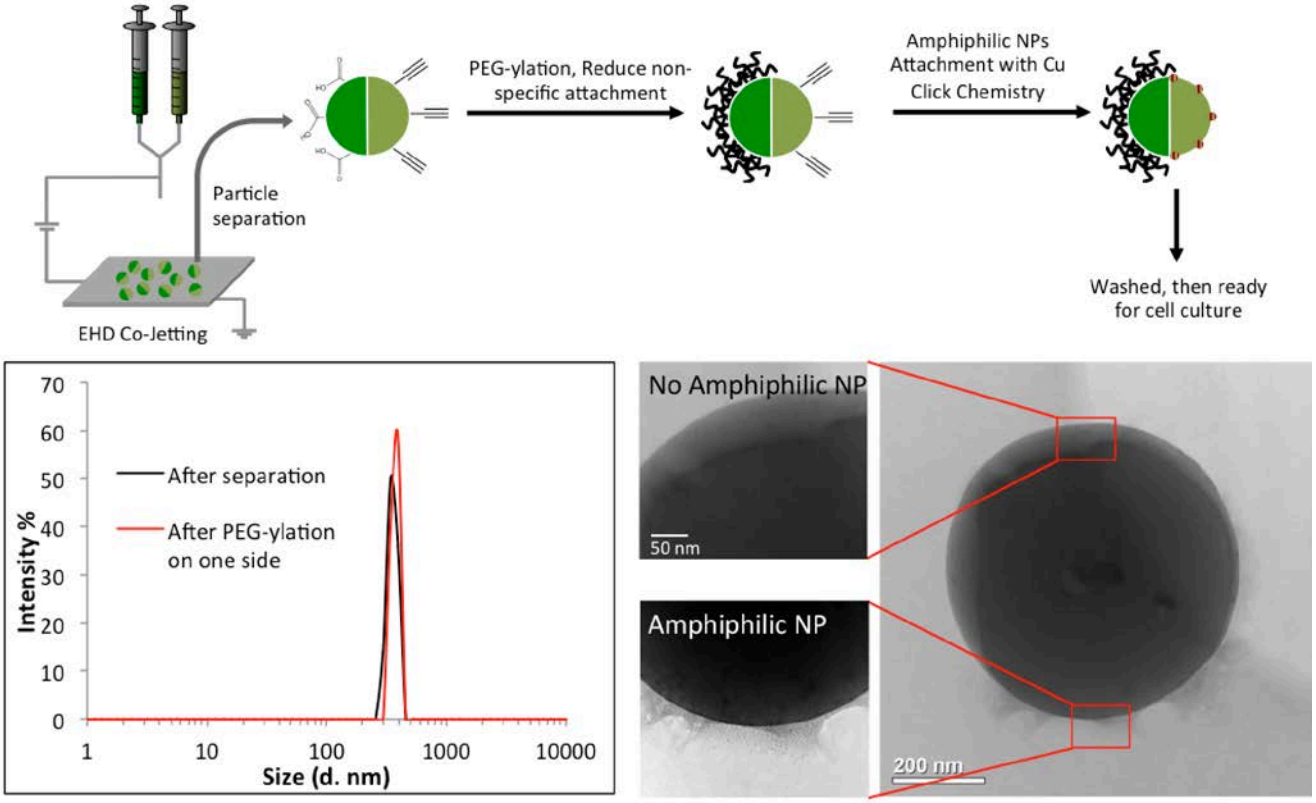

***Fig. 22**: Schematic for the processing of the Janus particles, their size distribution before and after preparation, and a TEM image of the selective immobilization of the rippled nanoparticles.*

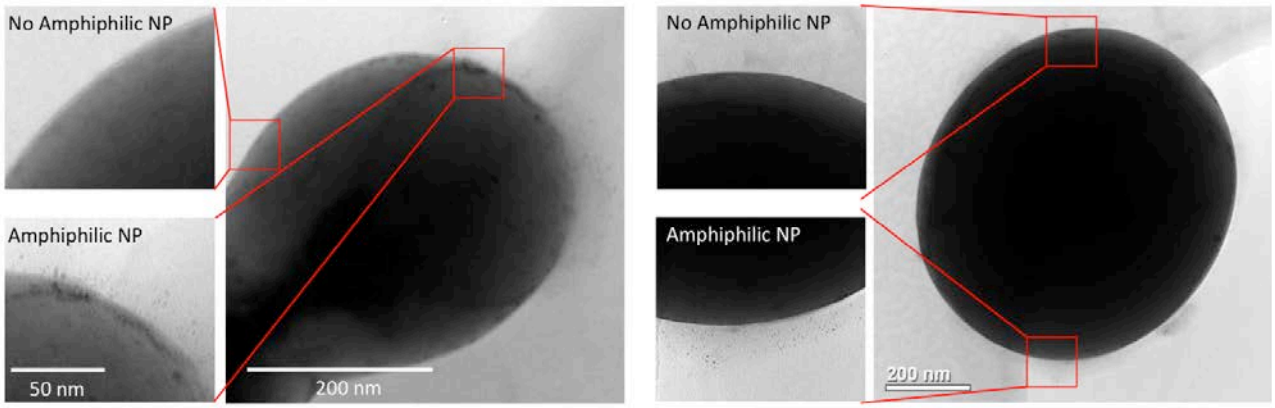

***Fig. 23**: Additional TEM image of the selective immobilization of the rippled nanoparticles on Janus vectors.*

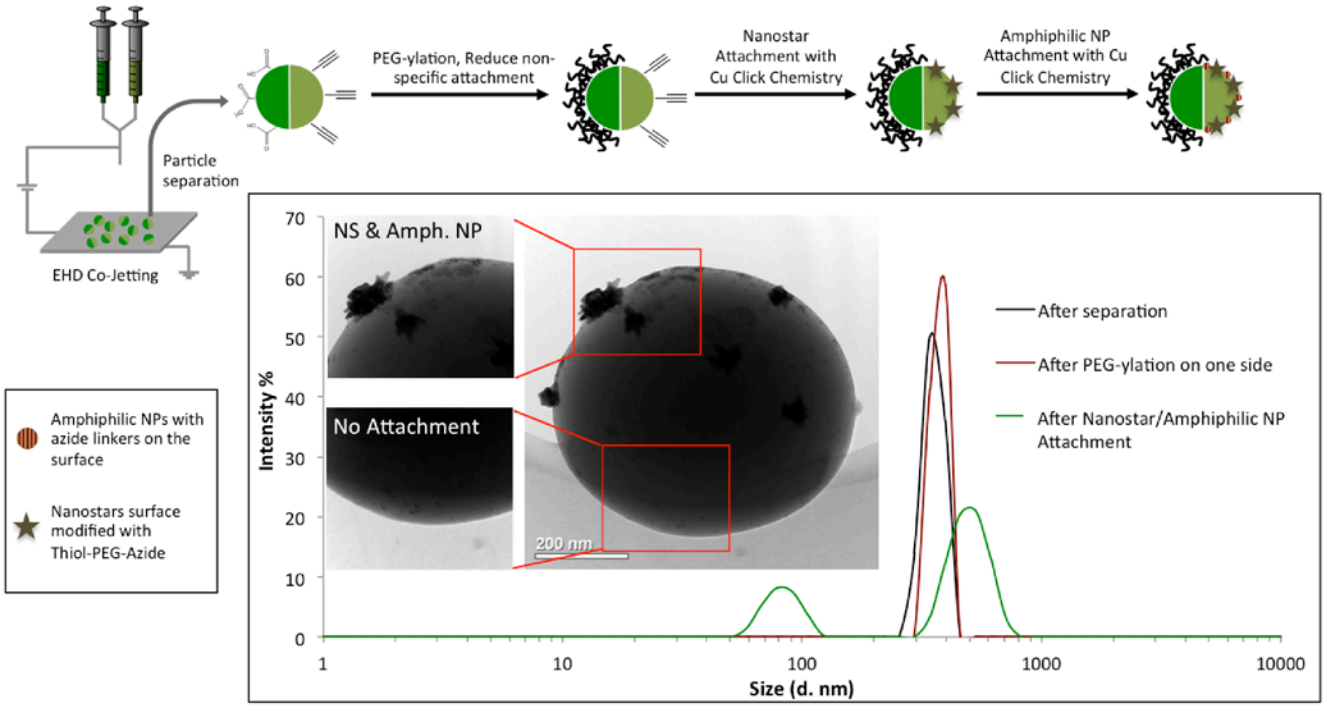

Fig. 24: *Schematic for the processing of the Janus particles, their size distribution before & after preparation, and a TEM image of the selective immobilization of nanostars and amphiphilic nanoparticles on one side of the Janus vectors.*

Finally, to demonstrate the selective immobilization of nanostars and amphiphilic nanoparticles on one hemisphere of Janus particles, a sequential set of chemistries was used. First, the same route described above for the immobilization of the gold nanostars was used, followed by several washes to remove all unreacted material. The Janus particles, now immobilized with nanostars, were then incubated with the amphiphilic nanoparticles for the second copper catalyzed click reaction (same procedure as above). The particles were then washed numerous times to remove the unreacted material. The schematic for the dual immobilization is outlined in **Figure 24**, as well as DLS measurements of the Janus particles after the separation, after PEG-ylation, and after the dual immobilization.

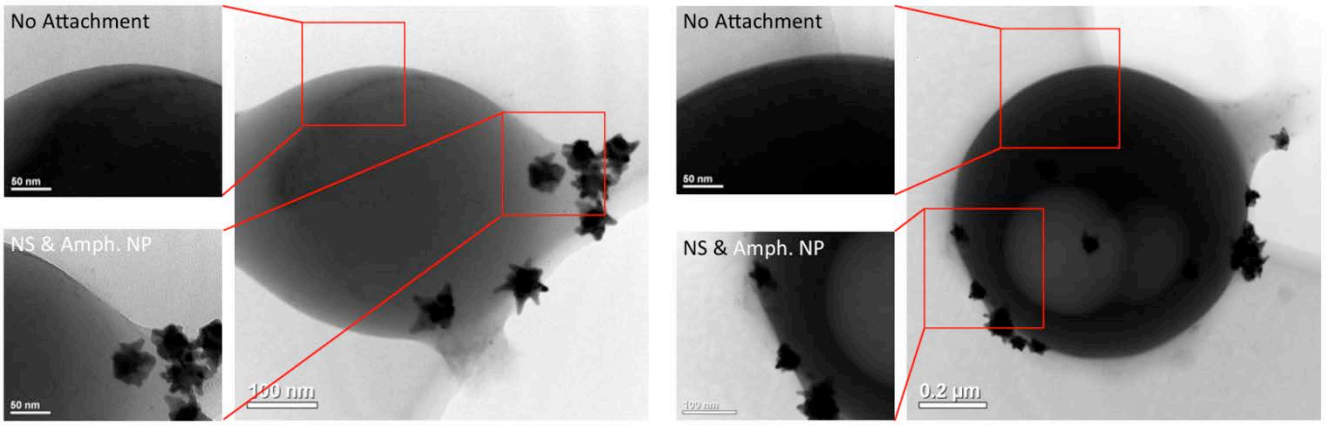

Fig. 25*: Additional TEM image of the selective immobilization of the nanostars and amphiphilic nanoparticles on one side of the Janus vectors.*

The size of the Janus particles increases slightly after PEG-ylation, and significantly more after the nanostar and rippled nanoparticle attachment. Additional TEM images confirming the attachment of the nanostars and the amphiphilic nanoparticles to one side of the Janus vectors is demonstrated above in **Figure 25**.

4. Fabrication of the Microfluidic Device

In the course of developing the whole SAVVY platform, each functional module as well as the functional interaction between two or more modules were optimized in a continuous way of process. This procedure is tightly associated with the stepwise integration of the modules forming a more and more complete SAVVY platform including the fluidic control station and the necessary interface. The cartridge has slide dimensions (75.5 mm x 25.5 mm) and contains Luer interfaces (**Figure 26**) for liquid supply and connection of several microfluidic modules or separate functional elements on chip. All interfaces except the first inlet have a special geometry with a big hole to reduce the risk of losing cells. The first inlet is also a Luer but with a standard

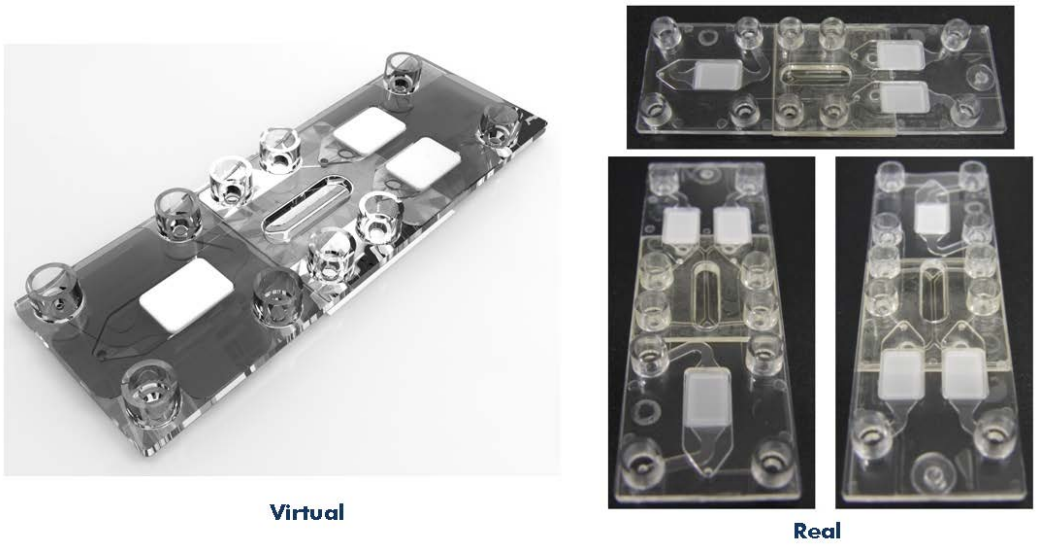

***Fig. 26**: Integrated SAVVY cartridge.*

changeover hole. This hole is smaller to support a pipette.

All parts of the cartridge are shown in **Figure 27**. Three membranes were assembled on the polymer chip. A bondfoil from top and below seals the channels except the holes for the quartz glass unit. The quartz glass unit is made out of two quartz glasses which are assembled with a double adhesive tape. This double sided adhesive tape creates and seals the channel as well. An additional double adhesive tape is necessary to mount the quartz glass unit to the main cartridge. This cartridge system was used for the Raman spectroscopy analysis of various cell types.

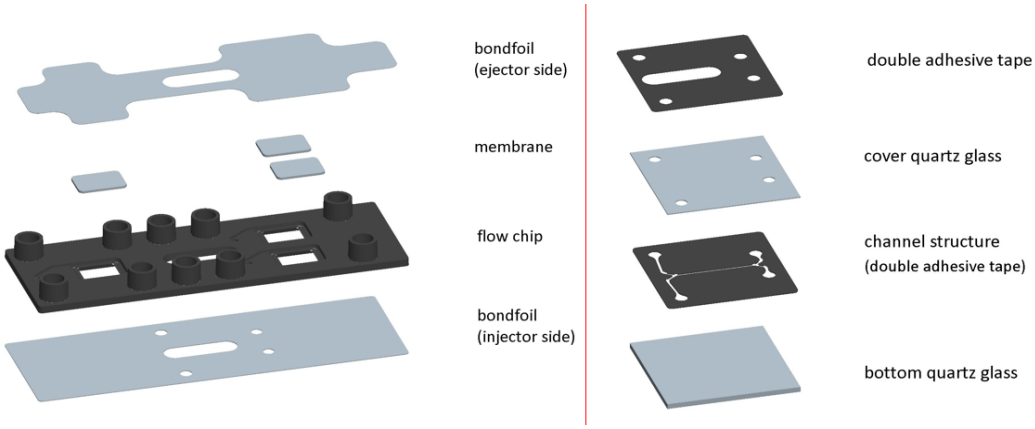

***Fig. 27**: Cartridge parts (quartz glass unit on the right side).*

5. Application of SAVVY Assemblies for SERS Detection

The assembled SAVVY vectors were tested to determine their compatibility with cells and their ability to be used for SERS signaling. Here, both the PS assemblies and the Janus PLGA-based assemblies were tested and both demonstrated the ability to produce SERS signaling with SERS active molecules and with HeLa cells.

For both systems, the particle characterization with cells produced heat maps of relevant peaks corresponding to the positions of SERS events. For our Raman spectroscopic studies, we refined our Raman spectroscopic imaging protocols, which have also been aided by the optimisation of the particle- and cell-based work. Raman spectroscopy imaging experiments were performed on a confocal Raman microscope from WITec alpha300R+. The Control FOUR 4.0 software was used for measurement and WITec Project FOUR 4.0 Plus for spectra processing. The Raman spectroscopy images were 30x30 µm with a 750 nm spatial resolution and a 1 sec integration time. Furthermore an in-house library in Python was used to estimate the pixel effects assuming that each image follows an additive model of the form where the intensity γ_{wp} for wave number w and pixel p can be decomposed (apart from the constant Y) into a component A_w specific to the wave number w (and common to all spectra), and a component B_p particular for a spectrum p but shared across wave numbers. The remaining intensity unexplained by the model is represented by the residuals e_{wp} [1]. Such a model was applied to each Raman image through the robust Median polish algorithm, where we can disentangle the effects of the image location (equivalent to the “pixel” or “spectral” effects) from the effects of the wave number dimension. The resulting residuals can be compared across images, and furthermore this same model can be applied to concatenated images.

$$y_{wp} = Y + A_w + B_p + e_{wp}$$

5.1 PS Assemblies

To begin, the SERS capability of PS-SAVVY particles (immobilized with gold nanostars and rippled nanoparticles) were tested (**Figure 28**). The SERS spectra of PS-SAVVY particles

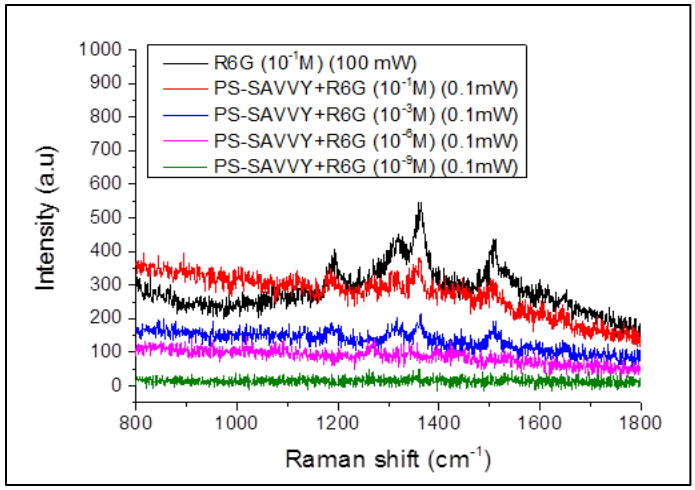

Fig. 28: *Raman and SERS spectra of PS-SAVVY particles with Rhodamine 6G (R6G). The Raman spectra were acquired with 100 mW on the sample using 10 sec integration time. SERS spectra were measured with 0.1 mW on the sample using 10 sec integration time.*

were measured with Rhodamine 6G (R6G) in various concentrations and SERS signals down to 10^{-3} M using 0.1 mW laser power on the samples with 10 sec integration time could be detected.

Once the SERS activity of the particles was established, the use of the PS-SAVVY particles for SERS detection in various cell types was explored. We have performed Raman spectroscopic analyses of HeLa cells, C2C12 cells and neural stem/progenitor cells (NSCs) in the presence of only nanostars, PS beads with nanostars, and PS beads with nanostars and striped nanoparticles (PS-SAVVY). **Figure 29** shows the SERS phenomena of PS-SAVVY reporter components in the presence of HeLa cells, C2C12 cells and neural progenitor cells (NSC).

Therefore, we have characterized the PS-SAVVY nanomaterials and their constituent components in the presence of two cells lines (i.e. HeLa and C2C12) as well as two human stem cell-derived neural cell types. In each of these cases, we successfully obtained cellular-nanoparticle attachment and SERS for each cell type. These studies embodied a characterisation of the interaction between the PS-SAVVY reporters and NSCs to better understand the adhesion process and optimise the coverage of the SERS reporter on the cells for the final application of SAVVY-enabled sorting using a live-imaging approach, incubating the reporters with the plated cells and acquiring fluorescent and bright-field images over the course of the experiment. Once the detection of SERS signalling was established for several different cell types and the optimum particle characterization for cell adhesion was determined, we moved on to using the developed system for the differentiation of distinct cells based on SERS signaling and downstream linear discriminant analysis.

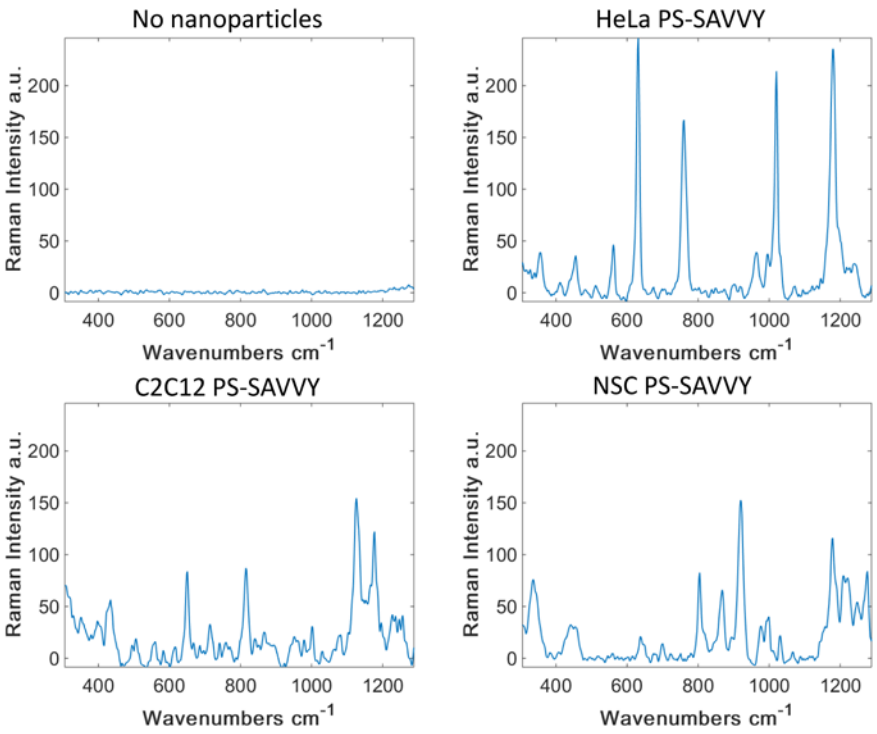

Fig. 29: *Raman scattering spectra showing SERS signaling of control cells (no nano-particles), PSf-RGD NSs in the presence of HeLa cells (top right), PSf-RGD NSs in the presence of C2C12 cells (bottom left) and PSf-RGD NSs in the presence of neural stem cells (NSC; bottom right).*

5.2 Janus Assemblies

Similar to the PS assemblies, the Janus assemblies were also first tested with a Raman reporter to determine their SERS activity, before testing them with cells. The Raman reporter 4-MBA at a concentration of $10x10^{-5}$ M under a 785 nm laser illumination was used with Janus particles. The nanostar-immobilized Janus particles were SERS active and contained the expected Raman signatures (**Figure 30**).

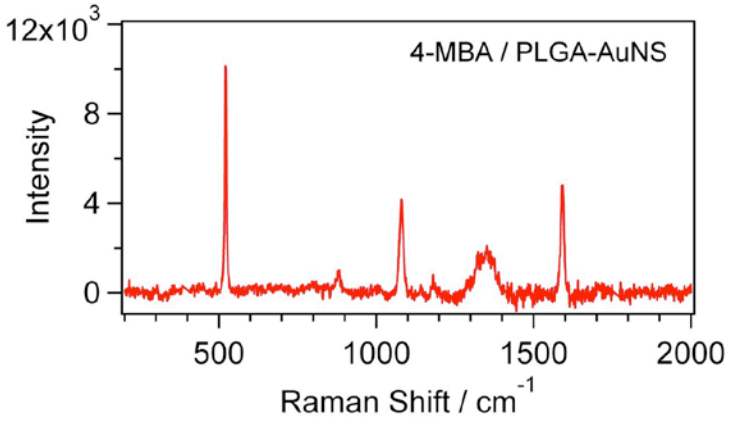

Fig. 30*: Raman spectra of Janus particles containing nanostars with 4-MBA as the SERS active molecule.*

Next, the particles were used to detect SERS signaling with HeLa cells. Here, the particles were incubated for 5 hours, after which they were analyzed with a confocal Raman spectroscope. While a distinct difference can be observed between the Janus particles with the nanostars versus the controls without any nanostars, the SERS activity was not as strong as those of the PS beads (**Figure 31**). In this case, this was to be expected since the particles did not contain the rippled nanoparticles and hence did not attach at the same concentrations. As such, these preliminary results were deemed to be promising and further testing for the differentiation of distinct cells based on SERS signaling and downstream linear discriminant analysis was done.

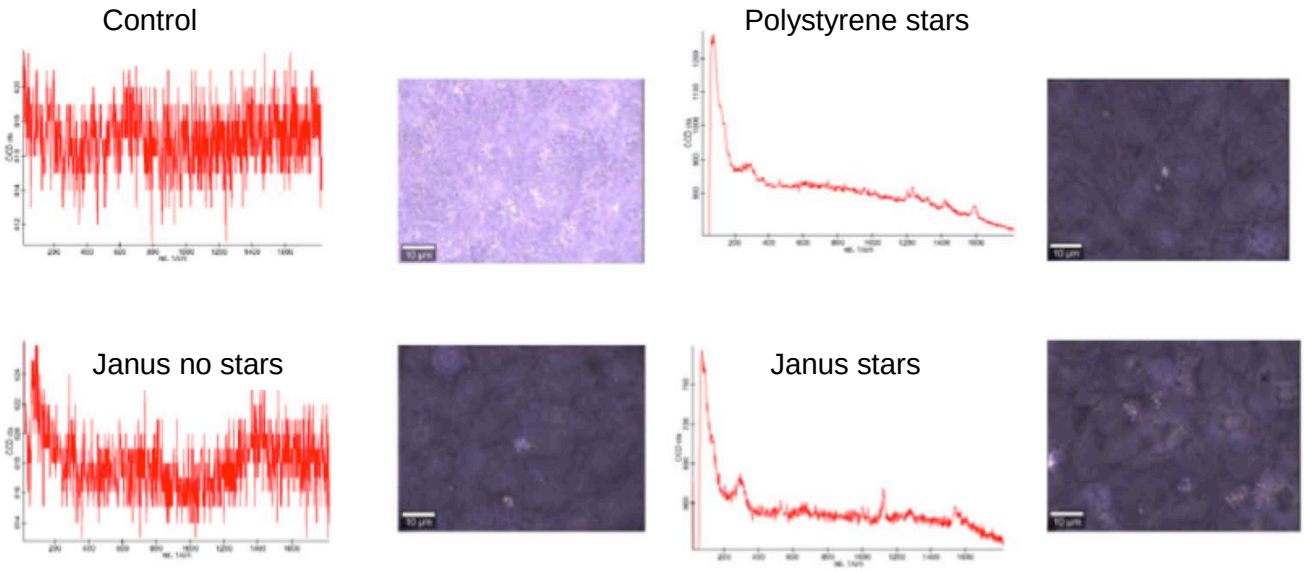

Fig. 31*: Raman analysis of cells for SERS activity after incubation with media (control), PS beads with nanostars and rippled NPs, Janus particles without surface modification, and Janus particles with nanostars.*

6. Use of SAVVY Assemblies for Cell Phenotyping

We have been able to create a comprehensive software package for phenotypic prediction/classification of SERS signals. The developed Python module can be used by our partners within SAVVY to analyze data from any Raman spectrum and the data outputs from SAVVY. With input from WITec, the phenotype classification software was integrated into the system through the WITec Control software. This software enables SERS spectra to be measured and classified in real-time through a hit quality index (HQI) between the sample and a set of reference spectra. To further extend the classification capability associated with the complex SERS signals, sophisticated algorithms were developed, which were incorporated into a general hyperspectral analysis toolbox to be employed in a high-performance computing environment. This toolbox is comprised of the Python module and iPython Notebooks to ensure reproducibility of all relevant analyses and allowed for the construction of a comprehensive library of signature spectra that can be exported to the phenotype classification software in order to ensure optimal classification performance.

The developed Raman spectroscopic framework has been implemented as a graphical user interface (GUI) under the WITec Control software. The software has been integrated into the SAVVY Raman microscope prototype that can classify SERS spectra according to the HQI

similarity index. Interaction and data exchange between the Raman control software and the phenotype classification software have thus been achieved.

The optimization of the classification capability associated with the complex SERS signals has been achieved by developing more sophisticated preprocessing and deconvolution algorithms, which can be analyzed through the Python module and then used to inform the phenotype classification software. Besides the usual baseline and background correction algorithms, a background removal algorithm has been created to further improve the usual baseline and background correction algorithms. After preprocessing, all images from the same cell type can be analyzed together.

Using these pooled images an endmember extraction algorithm (implemented in the Python module) can be applied to explore possible reference spectra. First both NFINDR and MCR-ALS on each cell type were applied separately to estimate a set of cell type-specific endmembers (**Figure 32**), and then we extracted one component from each cell type using all endmembers together, such that the dissimilarity is maximized (**Figure 33**). The resulting three spectra compose our signature library that can already be fed into the phenotype classification software.

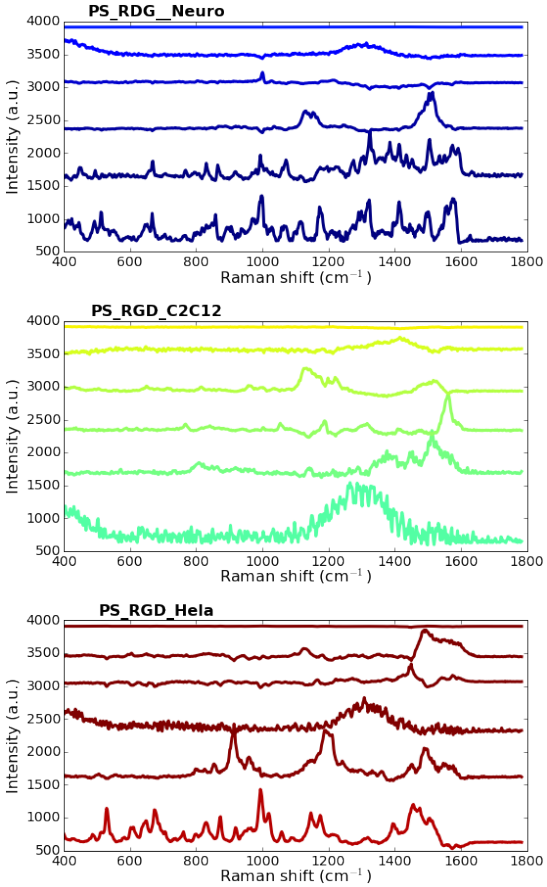

Fig. 32*: Pure components estimated using MCR-ALS on neural progenitor cells (top), C2C12 cells (middle) and HeLa cells (bottom) in the presence of polystyrene beads coated with nanostars. Each panel of pure components comprises an estimate of a signature library specific for each cell type.*

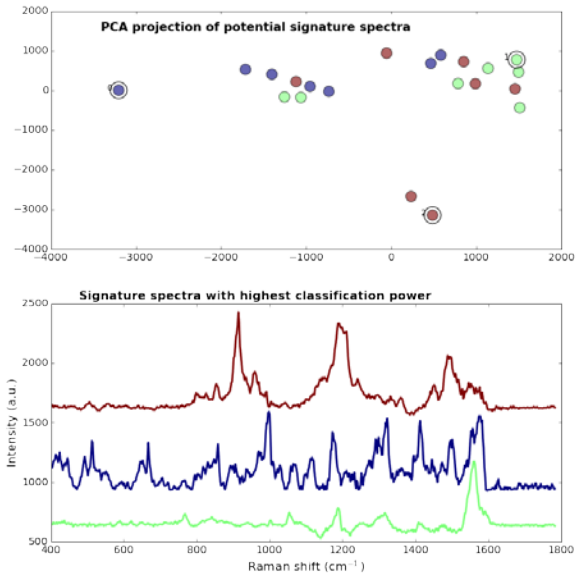

Fig. 33: *Estimation of reference spectra for classification using an HQI-based sorting. On the top panel we show the first two principal components for selected spectra from the cell-specific spectral library. The colours represent the cell type: HeLa cells in red, C2C12 cells in green and neural progenitor cells in blue. The circled elements are those that maximize the dissimilarity between all, and their spectra are shown in the bottom panel using the same colours.*

Using these reference spectra we are able to simulate the behavior of the actual HQI-based phenotype classification sorter. One example is shown below (**Figure 34**):

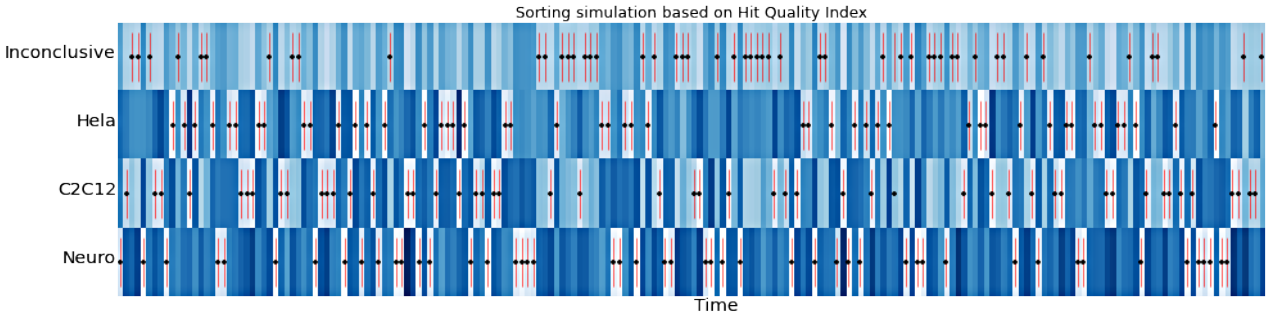

Fig. 34: *Simulation of an HQI-based sorting using the estimated reference spectra. The horizontal axis represents the temporal acquisition of sample spectra, which would then be compared to each reference signal (vertical axis). The distance between each sample (time point) and all references are shown as blue boxes (where darker blue means larger distance), and the inferred classification is represented by red lines. The true classification is shown as black dots.*

Once the phenotyping programing was well established, the SAVVY sorter was validated by performing detection of SERS signatures within the SAVVY chips of two different cell lines (HeLa cells and C2C12), using the polystyrene based reporters with rippled nanoparticles and nanostars (PS-SAVVY), the fully assembled Janus carriers based reporters (J-SAVVY) (**Figure 35**). A positive interaction was observed for both PS-SAVVY and J-SAVVY with both cell lines as previously established. Each cell line was associated with a unique SERS spectral signature that can be attributed to the various proteins and lipids comprising the cell membrane. We performed a time-series real-time acquisition that provided insights into the dynamics of the cell sorting. These results showed that SERS spectra could be measured over a longer time period, up to 100 sec.

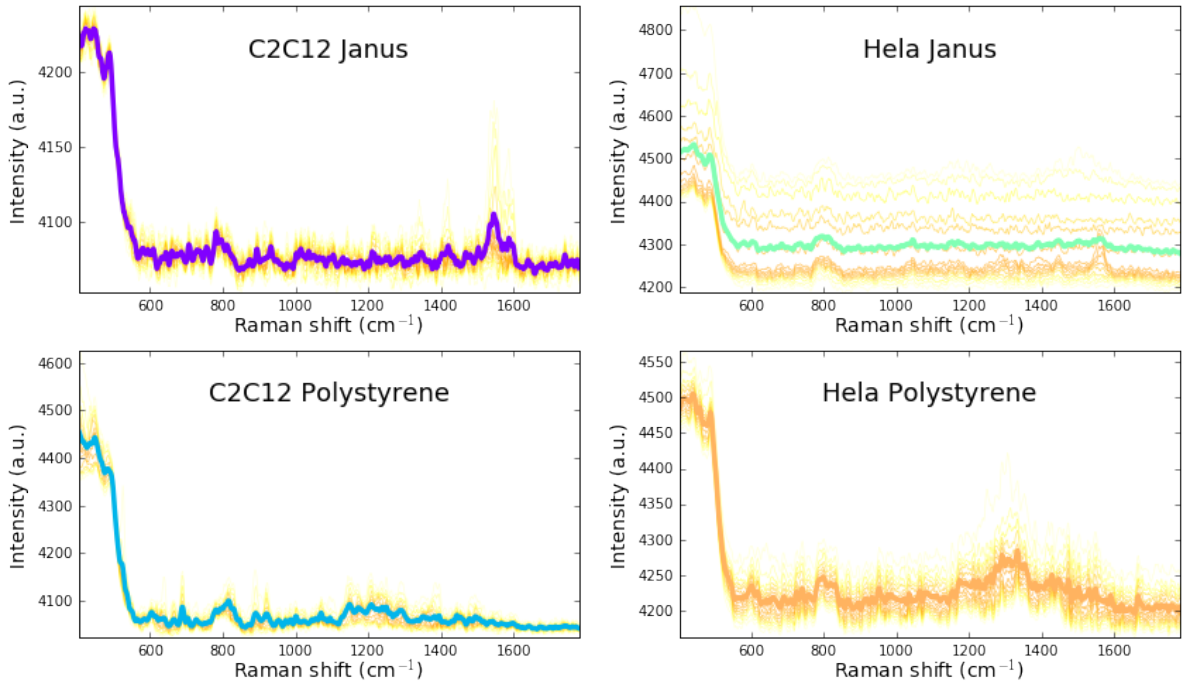

Fig. 35: *Spectral distribution of SERS signals measured from C2C12 and Hela cells using the PS-SAVVY and J-SAVVY particles. All measurements were performed inside the microfluidic chip with a power on the sample of 10 mW and 1 sec exposure time. The distributions comprise the mean spectra in bold plus their percentiles as yellow shading*

A two-component principal component analysis (PCA) integrated with linear discriminant analysis (LDA) was then performed on this data. The two first components from the PCA model accounted for most of the variance, and were able to discriminate the two cell lines. A supervised LDA classification further confirmed the differences between spectra (**Figure 36**). LDA scores of the C2C12 cell line were consistent for both the PS-SAVVY and J-SAVVY suggesting that the SERS signals have a degree of reproducibility. Interestingly the PC1 and PC2 scores for HeLa cells showed larger variability suggesting that the PS-SAVVY and J-SAVVY interact differently with the HeLa cells.

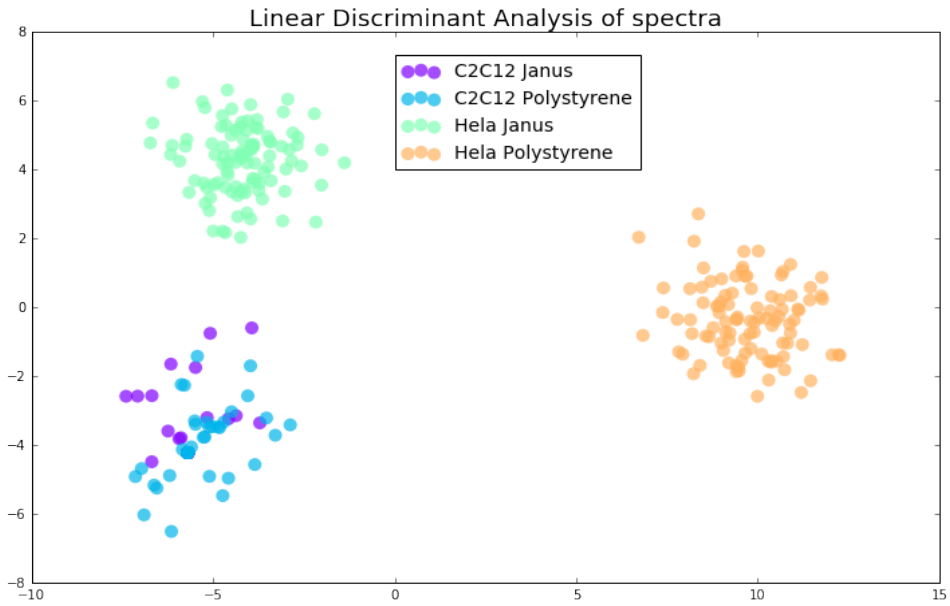

Fig. 36: *Projection of the first two components of the LDA using the combination of cell lines and reporters as possible classes in the supervised task.*

Conclusions

There are still no Raman spectroscopy-based techniques available on the market for cell sorting and signature-based characterization. However this project has validated and assessed the feasibility of such an approach. The SAVVY reporter components have been optimized by KIT and CICbio in 2015, which resulted in the validation of a prototype that was validated under investigations using the SAVVY instrument (assembled at Imperial, with input from WITec and ChipShop) which comprises a Raman spectroscope that can enable microfluidic characterization integrated with a phenotype classification software. The progress achieved within this project demonstrates that this approach is feasible for cell sorting and phenotyping and can undergo further optimization and studies to realize its translational potential.

References:

1. Serrano-Montes, A. B.; de Aberasturi, D. J.; Langer, J.; Giner-Casares, J. J.; Scarabelli, L.; Herrero, A.; Liz-Marzan, L. M., A General Method for Solvent Exchange of Plasmonic Nanoparticles and Self-Assembly into SERS-Active Monolayers. *Langmuir* **2015,** *31* (33), 9205-9213.
2. Sperling, R. A.; Parak, W. J., Surface modification, functionalization and bioconjugation of colloidal inorganic nanoparticles. *Philos T R Soc A* **2010,** *368* (1915), 1333-1383.
3. Roh, K. H.; Martin, D. C.; Lahann, J., Biphasic Janus particles with nanoscale anisotropy. *Nat Mater* **2005,** *4* (10), 759-763.
4. Bhaskar, S.; Pollock, K. M.; Yoshida, M.; Lahann, J., Towards Designer Microparticles: Simultaneous Control of Anisotropy, Shape, and Size. *Small* **2010,** *6* (3), 404-411.
5. Bhaskar, S.; Roh, K. H.; Jiang, X. W.; Baker, G. L.; Lahann, J., Spatioselective Modification of Bicompartmental Polymer Particles and Fibers via Huisgen 1,3-Dipolar Cycloaddition. *Macromol Rapid Comm* **2008,** *29* (20), 1655-1660.
6. Rahmani, S.; Villa, C. H.; Dishman, A. F.; Grabowski, M. E.; Pan, D. C.; Durmaz, H.; Misra, A. C.; Colon-Melendez, L.; Solomon, M. J.; Muzykantov, V. R.; Lahann, J., Long-circulating Janus nanoparticles made by electrohydrodynamic co-jetting for systemic drug delivery applications. *J Drug Target* **2015,** *23* (7-8), 750-8.

Contact information for SAVVY PIs / workpackage leaders:

KIT:
Prof. Dr. Jörg Lahann
Dr. Leonie Barner
Institute of Functional Interfaces
Karlsruhe Institute of Technology
Hermann-von-Helmholtz Platz 1
76344 Eggenstein-Leopoldshafen
Germany

EPFL:
Prof. Francesco Stellacci
Institute of Materials
École Polytechnique Fédérale de Lausanne
STI IMX SUNMIL
MXG 030
Station 12
1015 Lausanne
Switzerland

Universidad de Vigo:
Prof. David Posada
Facultad de Biología
Campus Universitario
Universidad de Vigo
36310 Vigo
Spain

Imperial College of Science, Technology and Medicine
Prof. Molly Stevens
Royal School of Mines
Imperial College of Science, Technology and Medicine
South Kensington Campus
Prince Consort Road
South Kensington
SW7 2AZ London
UK

Microfluidic ChipShop GmBH:
Dr. Holger Becker
Stockholmer Str. 20
07747 Jena
Germany

Asociacion Centro de Investigacion Cooperativa en Biomateriales
Prof. Luis Liz-Marzán
Ikerbasque Research Professor
Scientific Director
CIC biomaGUNE
Paseo de Miramón 182
20009 Donostia-San Sebastian
Spain

WITec Wissenschaftliche Instriumente und Technologie GmBH
Dr. Olaf Hollricher
WITec GmBH
Lise-Meitner-Str. 6
89081 Ulm
Germany